Batteries & Supercaps

Review
doi.org/10.1002/batt.202200275

Chemistry Europe
European Chemical Societies Publishing

www.batteries-supercaps.org

Special Collection

Shape-Memory Electrochemical Energy Storage Devices

Liangliang Yang[+],[a, c] Qingjiang Liu[+],[a, c] Youfa Liu,[a, c] Xiaoyang Chen,[a, c] Jinhao Luo,[a, c] and Yan Huang*[a, b, c]

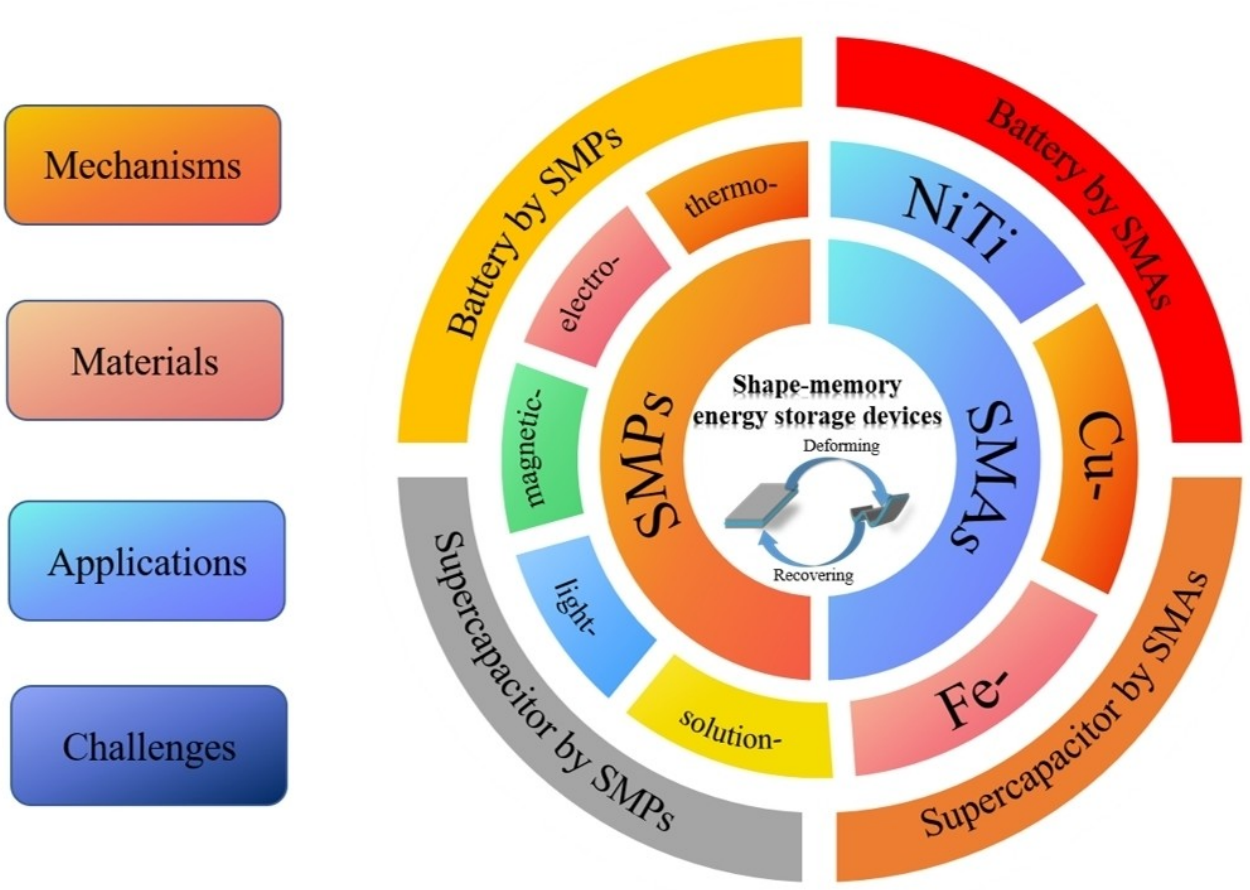

With the great development of rechargeable energy storage devices, security, operation, product life and quality of experience of these devices have attracted special attention. Aiming to resolve these challenges, smart electrochemical energy storage devices with shape memory function are being developed, because shape memory material can well serve as a detector. For example, if there is a risk during the use of a battery, it can convey the information in the form of shape and play the role of automatic protection simultaneously. In this review, we briefly introduce mechanisms and materials of shape memory, summarize the research progress of electrochemical energy storage devices with shape memory function in recent years, and the application of such energy storage devices. Furthermore, challenges and opportunities for the development of shape memory electrochemical devices are discussed.

1. Introduction

Under the influence of global warming, non-renewable fossil energy consumption etc., energy dilemma has become a widespread concern. To resolve the enormous issue of energy consumption and preserve the environment, most countries have decided to adjust their energy consumption configuration. Therefore, energy storage devices play a key role in daily life and societal pursuit.[1–8] As shown in Figure 1(a), they mainly include batteries and supercapacitors. Due to the widespread use of these equipment, their security, operational stability, product life are fundamental to achieve satisfied quality of experience, and they have drawn increasing attention.[9,10] Although these energy storage devices are often equipped with management systems with control and feedback modules, potential risks of their internal electrochemical reactions are still disturbing. In addition, they may be subjected to different degrees of external force, such as long-term deformation and accident damage, which seriously damages the stability and service life.[11–13] Therefore, researchers incorporate smart materials into flexible electrochemical energy storage devices that can respond to stimuli and adapt themselves to minimize potential risks, so as to prolong the service life and improve their stability and safety.[14–20]

Smart materials are stimulation-responsive materials with special functions that can respond to external stimuli.[16] Shape memory material is a typical smart material, which can sense the change of its own environment and make corresponding response to the change. In other words, it can remember initial shape and fix specific temporary shape when appropriate. Subsequently, when stimulated by external stimuli (such as heat, light, electricity, magnetism, solvent, humidity, etc.), it can spontaneously transform from temporary shape to initial shape, as shown in Figure 1(b). Shape memory materials exhibit a series of intelligent response characteristics such as self-perception, self-regulation and self-adaptation.[21–24] To solve the external mechanical damage and avoid permanent loss caused by severe deformation, scientists have well combined shape memory materials with energy storage devices. For instance, Hao et al.[25] reported a fluid-free, passive thermal regulator that stabilized battery temperature in extreme environment. Shape memory alloys (SMAs) was used to integrate two nonlinearities (i.e., solid-state phase transformation and interfacial thermal contact conductance) into the device topology to realize the control of thermal management. Zhang et al.[26] proposed a novel internal short circuit (ISCr) trigger method based on shape memory effect of SMAs (Figure 1c). The self-regulation function of shape memory materials was used to monitor and thus ultimately achieve the purpose of improving battery safety. However, these combinations were only utilized in parallel space. Researchers began to explore a better combination of shape memory material and electrochemical energy storage in a single device, and have achieved many progresses but without systematic summarization so far.

Therefore, the aim of this article is to summarize the important progress in the emerging field of shape-memory electrochemical energy storage devices and put forward challenges and prospects. First, we summarize the working mechanism and classification of shape memory materials. Then, we describe some specific design schemes. This is followed by their application in real situations. To close, the challenges and prospects of this rapidly developing field are briefly introduced.

[a] L. Yang,[+] Q. Liu,[+] Y. Liu, X. Chen, J. Luo, Prof. Y. Huang
Sauvage Laboratory for Smart Materials, School of Materials Science and Engineering
Harbin Institute of Technology, Shenzhen
Shenzhen 518055, P. R. China
E-mail: yanhuanglib@hit.edu.cn
[b] Prof. Y. Huang
Key Laboratory of Advanced Welding and Joining
Harbin Institute of Technology, Harbin
Harbin 150001, P. R. China
[c] L. Yang,[+] Q. Liu,[+] Y. Liu, X. Chen, J. Luo, Prof. Y. Huang
Shenzhen Key Laboratory of Flexible Printed Electronics Technology
Harbin Institute of Technology, Shenzhen
Shenzhen 518055, P. R. China
[+] Liangliang Yang and Qingjiang Liu contributed equally to this work.
Special Collection An invited contribution to a Special Collection on IV Symposium on Advanced Energy Storage

2. Shape Memory Materials

Shape memory materials are new functional materials developed from 1950s. These materials include crystals associated with martensitic transformation, and polymers through physical excitation such as glassy transition.[21]

2.1. Shape memory effect

In crystalline materials, SMAs are featured by four characteristic temperatures, namely austenite starts temperature (A_s), austen-

ite finish temperature (A_f), martensite starts temperature (M_s) and martensite finish temperature (M_f). Shape memory effect of SMAs is shown in Figure 2(a and b): martensite transformation will occur after cooling from high temperature, while martensite will become austenite after heating. Reversible transformation occurs after deformation, and the shape returns to the origin is called one-way shape memory effect. Materials which 'remember' the shape of the origin phase, and once again cooling can restore the shape of martensite deformation, are known as the two-way shape memory effect.[23,24,28] Due to the limitation of crystallography and the order of parent phase, the only way of atom migration during reversible transformation is to recover the original shape and phase.[21,28]

In polymer materials, shape memory polymers (SMPs) present a permanent shape at room temperature. When the temperature reaches the transition temperature (T_{trans}), the shape of the material can deform, and retain the deformed shape after cooling down. In addition, the original shape of the material can be restored by increasing the temperature.[29] When temperature is above T_{trans}, the original shape of the polymer is three-dimensionally chain cross-linked or entangled into a fixed shape. After high temperature deformation, the polymer exhibits a transition chain structure. When cooled down to below T_{trans} the shape of polymer remains unchanged. Then heated to T_{trans}, SMPs restore the chain structure and return to the original shape. The shapes at various intermediate states are reversible with temperature.[24,30]

Thermodynamic behavior of SMPs was carried out using thermoviscoelastic model. The molecular chain can be viewed as a little spring (Figure 2c). The spring has a short diameter but long length, and wraps around each other when agitated. At room temperature, the entropy of SMP is higher due to the arbitrary distribution of the spring. As the temperature increases, the mobility of polymer increases, forming thermoviscoelasticity. The spring can be elongated and oriented by external forces, thereby orientation can reduce the entropy of polymers. If the temperature is lowered without changing the external force, the polymer thermoviscoelasticity will be lost and its molecular motion is reduced, by which the spring cannot return to its original shape. During this process, the stress is stored in the spring as elastic potential energy. When the temperature rises again, the spring releases the stored elastic potential energy, generating thermoviscoelasticity.[31]

At the same time, the phase transition theory also analyzes the morphological memory properties of SMPs. The phase composition of SMPs can be divided into frozen phase and active phase. The frozen phase occurs when the enthalpy of the substance changes and the molecular chains are stretched or rotated to keep its internal structure remains the same. In the frozen phase, further conformational motion of the molecular chains is impossible. In contrast, the active phase consists of dynamic bonds. molecular chains can deform, rotate, stretch and compress. The freezing stage is dominated by glass phase. When the polymer changes from glass state to rubber state, part of frozen phase changes into active phase. As the temperature decreases, the active phase transitions to the frozen phase and the stress becomes localized. In contract, as the temperature rises, the frozen phase transforms into the

Liangliang Yang is a postgraduate student in Harbin Institute of Technology, Shenzhen. He mainly engages in the study of high-performance aqueous batteries.

Xiaoyang Chen is a postgraduate student in Harbin Institute of Technology, Shenzhen. He mainly engages in the study of synthesis and application of aqueous zinc-ion battery materials.

Qingjiang Liu is a postgraduate student in Harbin Institute of Technology, Shenzhen. He mainly engages in the study of smart flexible energy storage devices.

Jinhao Luo is a postgraduate student in Harbin Institute of Technology, Shenzhen. He mainly engages in the study of hydrogel electrolytes of aqueous zinc-ion batteries.

Youfa Liu is currently a PhD student in Harbin Institute of Technology, Shenzhen. His research mainly focuses on high- performance thermogalvanic cells and ion thermoelectric materials.

Yan Huang received her PhD degree in University of Rochester (USA) in 2013. Then she moved to City University of Hong Kong (China) as a post-doctoral fellow, followed by a Research Fellow. She has been a professor in School of Materials Science and Engineering at Harbin Institute of Technology, Shenzhen (China) since 2017. Her research interests include aqueous energy and application in flexible/wearable electronics.

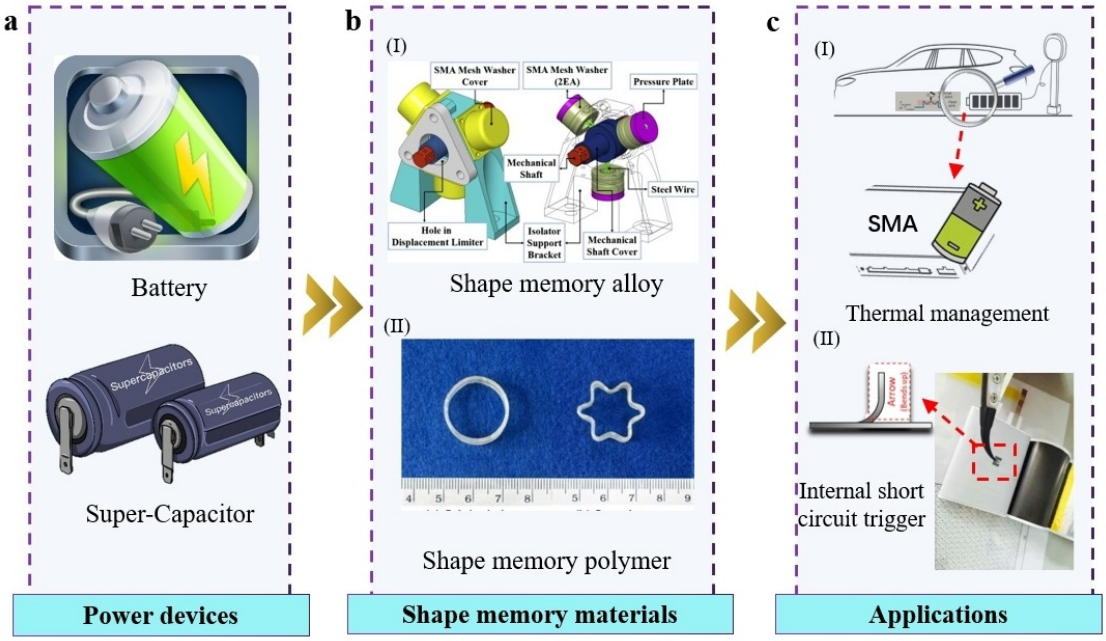

Figure 1. a) Common electrochemical energy storage devices. b) (I) Shape memory alloy. Reproduced with permission from Ref. [27]. Copyright (2015) Elsevier. (II) Shape memory polymer. Reproduced with permission from Ref. [23]. Copyright (2012) Elsevier. c) (I) The SMAs-actuated thermal regulator. (II) SMA ISCr trigger. Reproduced with permission from Ref. [26]. Copyright (2017) The Electrochemical Society.

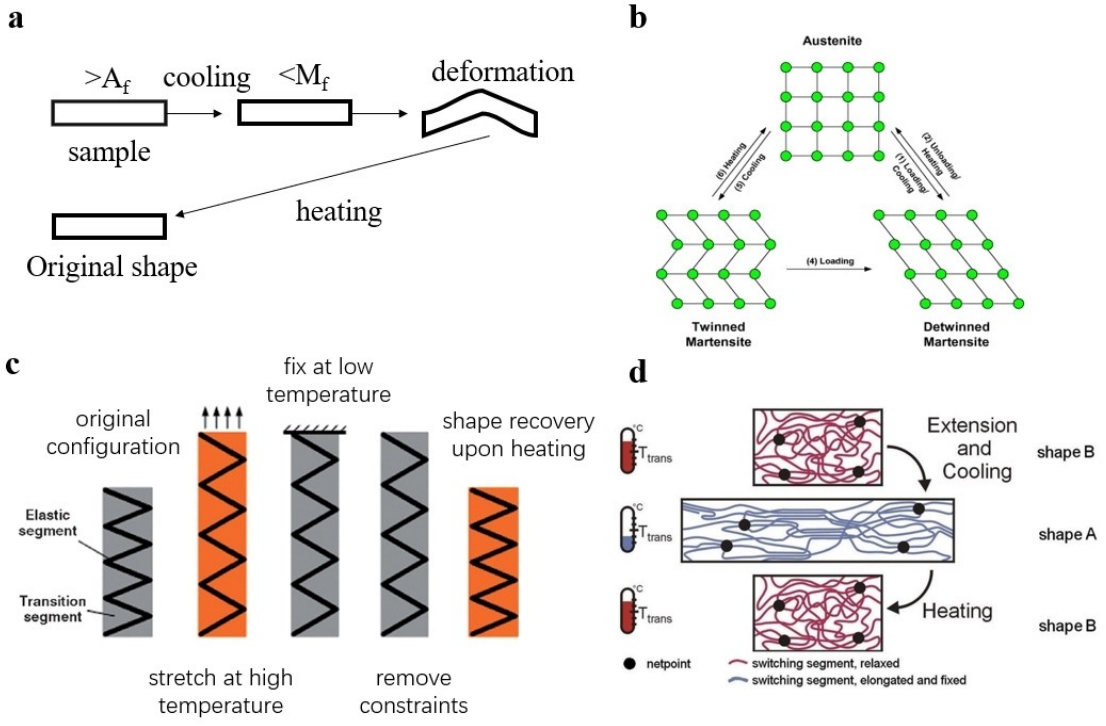

Figure 2. a) Shape memory effect of SMAs. b) Change in lattice structure. Reproduced with permission from Ref. [23]. Copyright (2012) Elsevier. c) Thermoviscoelastic model illustration of the mechanism of SMPs. Reproduced with permission from Ref. [32]. Copyright (2010) Elsevier. d) Phase transition illustration of the mechanism of SMPs. Reproduced with permission from Ref. [33]. Copyright (2007) Elsevier.

active phase, releasing the stored stress. The transformation of frozen and activated phases reflects glass transitions in thermodynamic cycles and accounts for stress storage and release in shape memory (Figure 2d).[34,35]

2.2. Shape memory alloys

2.2.1. Ni-Ti alloys

Although the invention of shape-memory effect can trace back to the early 1950s, the engineering significance of SMAs was not well recognized until the effect discovered in the near atomic ratio Ni–Ti alloys (Nitinol) in decade later.[21,28] Nitinol have been well recognized for their rich phase transition, excellent shape memory and pseudo-elasticity, good mechanical properties, corrosion resistance, biocompatibility and high damping properties. For the toxicity of Ni–Ti alloy, because of the existence of nickel, the oxide film on the surface is a good protection, and the addition of other elements also has the effect of restricting the outflow of nickel elements to inhibit the toxicity. They are the most widely used shape memory materials at present, which has been applied in aerospace, aviation, machinery, electronics, transportation, building energy, biomedical and other fields. In addition, the shape memory temperature of Nitinol is strictly controlled by the content. The atomic ratio of Ni to Ti and the content of C element in the composition can affect the phase transition temperature. The addition of a third element has also a significant effect. In other words, the required shape memory temperature can be achieved by changing the composition of the alloy, which will facilitate the expansion of its wide range of applications.[36,37]

Recently, based on the Ni–Ti alloys, adding other elements ternary alloy have also been developed. Adding Cu to the binary Ni–Ti SMAs has negligible effect on the martensitic transformation temperature but changes the transformation order of phases. Compared with binary Ni–Ti alloys, Ni–Ti–Cu is a good pseudo-elastic material because of its smaller transformation hysteresis. Adding Nb to Ni–Ti SMAs depresses the M_s temperature and separates the A_s from M_s as far as 150 K. The M_s temperature of Ni–Ti alloy is generally lower than 100 K, and the operating temperature of memory alloy device is determined by the M_s. In addition, the phase transition temperature can also be increased by adding noble metal elements Pd, Au and Pt instead of Ni or adding Hf and Zr instead of Ti.[21,24,28]

2.2.2. Cu-based alloys

Cu-based shape memory alloys are also called β phase alloys because their parent phase is body-centered cubic structure. They have many advantages, such as excellent shape memory performance, low price, good electric and thermal conductivity, and wide adjustable range of phase transition temperature.[21,28] Therefore, they are used in electronic communication, machinery manufacturing, civil construction, and daily life.[38] They can be mainly divided into Cu–Al and Cu–Zn series, among which Cu–Al–Ni, Cu–Al-Mn and Cu–Zn–Al have the most practical value. Cu–Al–Ni alloys have more excellent thermostability and higher operating temperature than other Cu-based SMAs. At the same time, their workability can be significantly improved by adding other elements.[39]

2.2.3. Fe-based alloys

According to different types of martensitic transformation, Fe-based shape memory alloys can be classified as Fe–Mn–Si, Fe–Ni–Co, Fe–Pt and Fe–Pd systemsalloy.[21,28] Among them, Fe–Mn–Si is the most widely used Fe-based SMAs in life due to moderate transformation temperature, excellent mechanical and machining properties, and low raw material price compared with above-mentioned Ni–Ti and Cu-based alloys. They have been utilized as pipeline or mechanical connectors, installation fixtures and temperature sensing parts of safety devices.[40]

2.3. Shape memory polymers

SMPs can adjust its parameters under external stimuli to return to the initial state with different mechanism from that of SMAs. For SMPs, there are many kinds of SMPs, such as PVA, PEG and others. If they are used in the field of wearable electronics, we should select a non-toxic and biocompatible polymer. Degradable SMAs and SMPs should be one solution to environment. As shown in Figure 3, they also can be divided into thermo-, electro-, magnetic-induced and light-, solution-driven SMPs.[29] Compared with SMAs, SMPs has the characteristics of easy processing, good printing suitability, corrosion resistance and so on.[33,41,42] Therefore, researchers have paid great attention to them since being discovered.

2.3.1. Thermo-induced SMPs

Thermo-induced SMPs have shape memory and recovery process due to temperature change caused by heat source stimulation either direct or non-contact heating such as infrared light irradiation, applying electric field or changing magnetic field.[29,33,41,42] Zhang et al.[43] reported a heat-responsive hydrogel with dual-network by using physically cross-linked elastin-like polypeptides (ELP) and chemically cross-linked polyacrylamide (PAM). The hydrogel retains its new shape at a high temperature of 55 °C. While temperature decrease to 20 °C, the hydrogel can repetitively restore to its original shape fast. Chen et al.[44] developed a facile synthesis approach through the formation of multiple H-bonds between polyvinyl alcohol (PVA) and tannic acid (TA), resulting in coagulation at high temperature and easy gelation at room temperature. With the characteristics of fast response and high repeatability, thermo-induced SMPs have broad application prospects.[43,44]

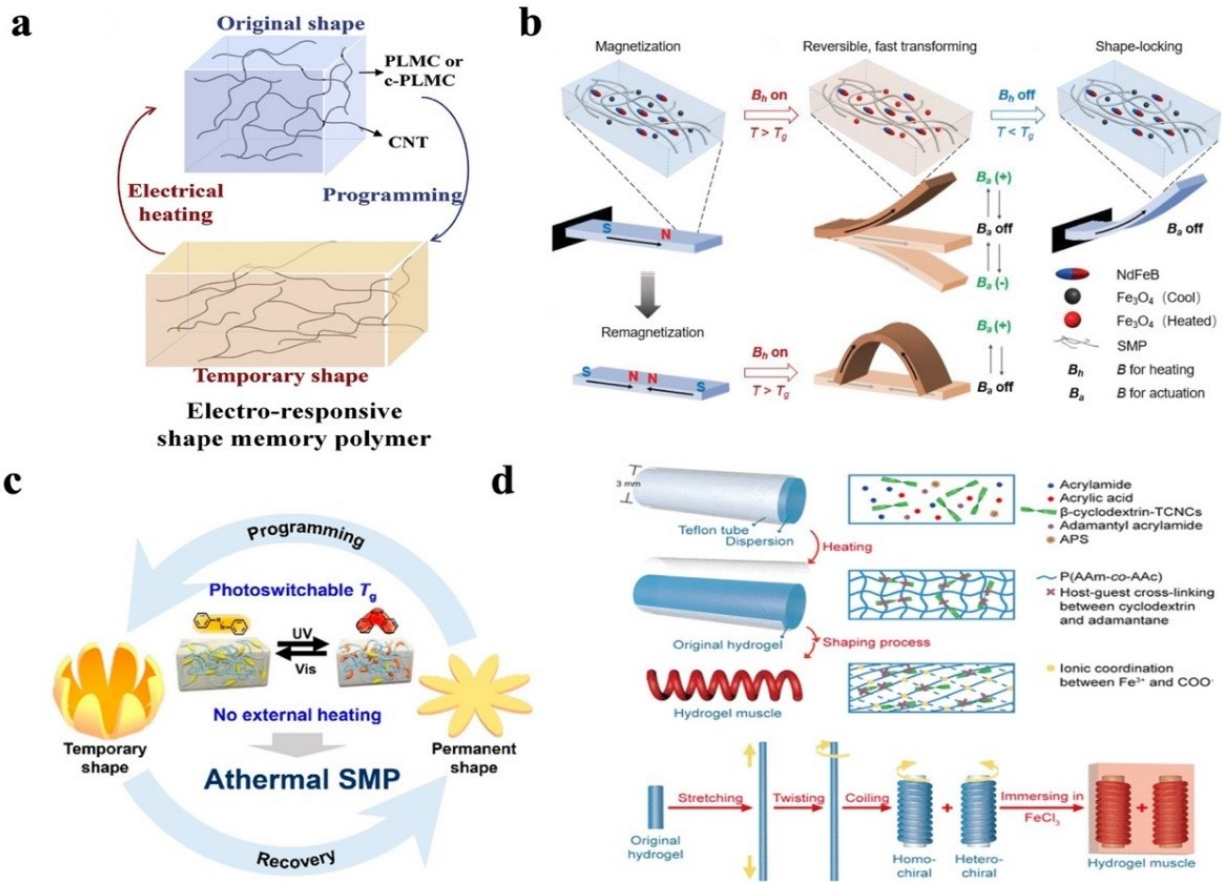

Figure 3. a) Electro-induced SMPs. Reproduced with permission from Ref. [45]. Copyright (2019) Elsevier. b) Magnetic-induced SMPs. Reproduced with permission from Ref. [49]. Copyright (2020) Wiley-VCH. c) Light-driven SMPs. Reproduced with permission from Ref. [52]. Copyright (2019) American Chemical Society. d) Solution-driven SMPs. Reproduced with permission from Ref. [54]. Copyright (2021) American Chemical Society.

2.3.2. Electro-induced SMPs

Electrically induced SMPs are a kind of SMPs that form a conductive network between conductive fillers by adding an appropriate amount of conductive materials to the SMPS matrix. When the heat produced by current rises the temperature to higher than $T_{trans,}$ the shape memory or recovery behavior occurs.[29] Common conductive materials include graphene, graphite, carbon nanotubes (CNTs), conductive metal particles and conductive polymers (Figure 3a).[45] Lu et al.[46] synthesized three-dimensional self-assembled multi-walled CNTs in a hydrophilic polycarbonate film. The conductive CNTs were combined with the SMP to facilitate resistance heating induced drive in SMPs. Wang et al.[47] developed a three-dimensional silver nanowires conductive network on melamine foam (MF) using shape memory epoxy resin by immersion coating and vacuum perfusion. Electro-induced SMPs have advantages of high electric conductivity, convenient heat generation, remote drive and fast heat conduction, therefore have a broad application prospect in fields such as electronic communications.

2.3.3. Magnetic-induced SMPs

Magnetic-driven SMPs is SMPs adding magnetic particles. In additional magnetic field or under the action of electromagnetic field, the magnetic particles circulate with the reciprocating motion, and friction and collision between the particles produce heat, which makes the material temperature rises. When it reaches the shape transition temperature, the shape memory effect is triggered.[29] Zhang et al.[48] directly added Fe_3O_4 nano-powder to Nafion solution as a functional filler to obtain a composite fiber with shape memory and self-heating functions, in which Fe_3O_4 particles can be heated by a distant alternating magnetic field. Ze et al.[49] reported a novel magnetic-driven SMP with reprogrammable, free, fast and reversible actuation and shape locking. Its main components are two different magnetic particles of Fe_3O_4 and NdFeB in the amorphous SMP material. The Fe_3O_4 particles can be induction heated by a high frequency alternating electromagnetic field, so that shape locking and unlocking of the target can be achieved. To achieve programmable deformation under a driving magnetic field, NdFeB particles are magnetized with a predetermined magnetization distribution (Figure 3b). Magnetic-driven SMPs can solve the problem of traditional thermo-

and electro-induced shape memory polymers, but at the same time, have some shortcomings such as low controllability, low heat generation efficiency and long recovery time.

2.3.4. Light-driven SMPs

Light-driven SMPs can realize shape memory and recovery under the stimulation of light source. Compared with thermo-induced shape memory polymers, they have the characteristics of non-contact, instance and cleanliness. Zhang et al.[50] demonstrated that the polymer exhibits photo-controllable shape memory capability and fast optical repair by chemically cross-linking crystals and loading a small amount of gold nanoparticles (AuNPs) on them under the effect of surface plasmon resonance of AuNPs. On the one hand, the photothermal effect performs shape memory by adjusting the temperature of the crystal phase; on the other hand, it activates damage repair due to the melting and recrystallization of the crystal. Zhang et al.[51] embedded Au nanorods (AuNRs) to polyvinyl alcohol (PVA), by changing the polarization direction of the incident laser at 785 nm relative to the tensile direction of the film, the amplitude of the longitudinal surface plasmon resonance of AuNRs can be continuously changed, and the glass transition of the local temperature relative to the PVA matrix, and the temperature of the composites increases. Thus, by adjusting the polarization of the laser while holding all other things constant, the process of temporary to permanent shape restoration of composites can occur to varying degrees. Programmable shape recovery is further promoted due to the instantaneous, precise and spatiotemporal manipulation of light. This strategy may be an important part of next-generation sophisticated medical devices and soft robots (Figure 3c).[52]

2.3.5. Solution-driven SMPs

The shape memory effect of solution-driven SMPs is stimulated by the change of the chemical medium in the surrounding environment. There are many solution-driven ways, such as pH value change, balance ion replacement, redox reaction, phase transition reaction, chelation reaction and so on. Chen et al.[53] synthesized a high sensitivity to pH polymer by adding a pyridine ring into the polyurethane main chain. Cui et al.[54] proposed a plain and valid strategy for the preparation of tendril hydrogel artificial muscles inspired by plant tendrils, which achieved large stroke, high working capacity and shape memory properties. Because the twisting and helical directions of hydrogel were chiral, hydrogel muscles formed two kinds of helical structures: chiral and anti-chiral muscles. These two types of muscle exhibited opposite properties in response to solvent stimulation. The reverse chiral muscles contracted rapidly in ethanol and stretched to recover in water. The chiral muscles elongated in ethanol and resumed contraction in water (Figure 3d).

3. Electrochemical Devices with Shape Memory Function

Recently, functional wearable electronic devices have been rapidly expanded with the development of modern industries and multidisciplinary fields such as big data of the Internet and artificial intelligence. During repetitive bending and folding, it is easy to cause the separation of components for energy storage devices, affect the electrochemical performance and even lead to short circuit. Thus, shape-memory energy storage devices as a type of intelligent device have attracted wide attention.

3.1. Electrochemical devices by SMAs

Ni–Ti SMAs possess ideal electrical conductivity and therefore can be applied as a current collector of electrochemical devices. It can change to original shape under mechanical deformation including drawing, bending, or twisting etc. The flexibility of Ni–Ti alloy has also become one of the choices of flexible energy storage devices. In addition, good biocompatibility has led to the application of shape memory energy storage devices based on Ni–Ti alloy in contact with human skin, such as textiles or watchbands mentioned later. Wang et al.[55] prepared a shape-memory fiber battery based on Ni–Ti wire, gelatin-borax composite electrolyte and stainless steel yarn (Figure 4a). The rechargeable zinc ion battery was prepared by electro-depositing zinc on the wire, and it had good electrochemical performance against mechanical deformation. As shown in Figure 4(b), the battery can recover to the initial state, meanwhile maintained most electrochemical performance. Obviously, experimental verification shows that the original shape was restored in only 6 s after abundant deformation test (Figure 4c). Cho et al.[56] applied flexible Ni–Ti alloy as current collector to Li/S battery. At room temperature, Ni–Ti alloy was mainly composed of austenite phase. With the increase of charge-discharge cycles, Ni and Ti elements were dissolved in the electrolyte, and the utilization rate of S was reduced due to the reaction between S and dissolved Ni and Ti elements. In order to avoid this problem, the authors made new changes.[57] The Ni–Ti alloy was vulcanized at 80 kPa and high temperature to form sulfides with layered structure. It did not change significantly for the thermal and mechanical properties of the alloy, and a Li/S wire battery was prepared with hot vulcanized Ni–Ti alloy as cathode instead of current collector.

As another important electrochemical energy storage device, supercapacitor has the characteristics of high-power density, safety, long service life and fast charge and discharge capacity. Huang et al.[58] successfully manufactured a shape-memory supercapacitor (SMSC). As schematically illustrated in Figure 5(a)-(l), a Ni–Ti alloy wire is used as the current collecting base and matrix to respond to micro and large deformation, while MnO_2 and PPy have better electrochemical properties. This conclusion was confirmed in EIS tests before and after the deformation recovery cycle (Figure 5b). After up to 15 deforma-

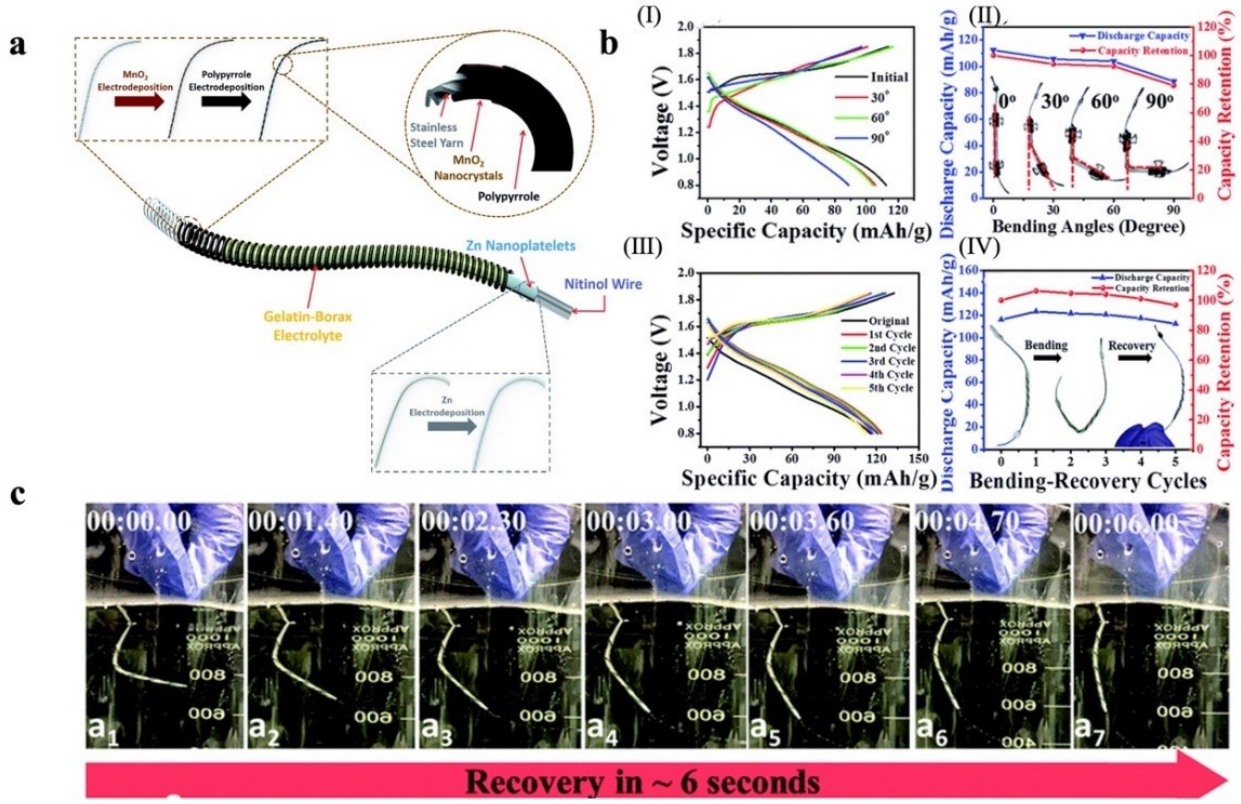

Figure 4. a) Schematic illustration of the assembly technology of the shape-memory wire battery. b) Mechanical flexibility and electrochemical performance of the shape-memory wire battery: (I) Charge - discharge curve of shape memory wire battery at different bending angles (II) Discharge capacity and capacity retention of the shape memory wire battery at different bending angles. (III) Charge - discharge curve of the battery tested continuously for 5 times in shape memory experiment tested at 2 C. (IV) Discharge capacity and capacity retention of the battery tested continuously for 5 times in shape memory experiment tested at 2 C. c) The rapid shape recovery process of shape memory battery in 45 °C water for 6 s. Reproduced with permission from Ref. [55]. Copyright (2018) Royal Society of Chemistry.

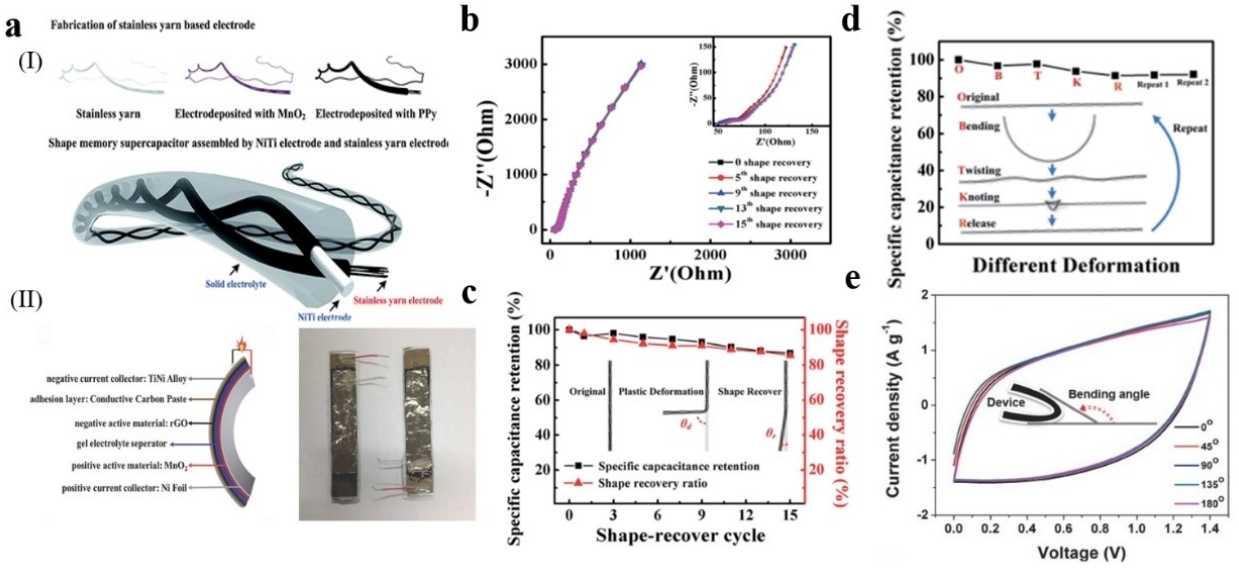

Figure 5. a) Shape-memory supercapacitor. (I) Schematic diagram showing the symmetric supercapacitor assembled from Ni–Ti alloy and stainless yarn. Reproduced with permission from Ref. [58]. Copyright (2016) Royal Society of Chemistry. (II) Schematic diagram of assembling a shape-memory asymmetric supercapacitor (SMASC). b) EIS spectra of before and after shape recovery under different cycles. c) The capacitance retention rate and shape recovery rate of SMSC before and after shape recovery under different cycles. d) Capacitance retention under various deformations. Reproduced with permission from Ref. [58]. Copyright (2016) Royal Society of Chemistry. e) CV curves of SMASC under different statical curvatures. Reproduced with permission from Ref. [59]. Copyright (2016) Wiley-VCH.

tion-recovery cycles, the shape recovery rate remained as high as 90% and the capacitance retention rate also showed satisfactory stability (Figure 5c). As shown in Figure 5(d), the GCD curve of SMSC maintained good symmetry in the deformation process of three cycles (bending/torsion/knotting/releasing). Liu et al.[59] prepared another supercapacitor with graphene coated on Ni–Ti alloy as negative electrode, ultra-thin MnO_2/Ni film as positive electrode, and gel as electrolyte and separator (Figure 5a-II). The static and dynamic bending tests verified that the prepared devices had good electrochemical performance and reliability. All CV curves maintained the origin shape even at over 180° (Figure 5e), demonstrating good electrochemical performance reliability. Combined with the work of Wang et al., Zhao et al.[60] prepared symmetrical supercapacitors by electrodeposition of polypyrrole onto Ni–Ti alloy. However, like the shape-memory battery mentioned above, Ni–Ti alloy still only acted as a current collector. If various mechanical behaviors are encountered, the separation of electrode materials and collector will make the energy storage devices fail. At the same time, Cu- and Fe-based SMAs have not been used in electrochemical energy storage devices. So, there is still a lot of work to be explored in these areas.

3.2. Electrochemical devices by SMPs

In order to incorporate into secondary batteries, scientists explored utilizing SMPs as solid electrolyte, so that the battery has the function of shape memory. Zhou et al.[61] developed a shape-memory solid polymer electrolyte (SSSPE) by reversible addition-fragmentation chain transfer polymerization of a ureidopyrimidinone (Upy) containing monomer and poly (ethylene glycol) methyl ether methacrylate (PEGMA) for high-performance lithium-ion batteries. Then, Jo et al.[62] conducted a similar work, in which a SSSPE was prepared with polyvinyl alcohol (PVA) as the main chain, PEG and UPy with epoxy-function as the side chains (Figure 6a-I). Jabbari et al.[63] reported a lithium-ion battery (LIB) with shape memory function induced by a SSSPE. The SSSPE was designed based on polyethylene oxide dimethacrylate (PEO-DMA) synthesized by one-step methylation of PEO and LiTFSI as Li salt (Figure 6a-II). As a solid electrolyte, SMPs must have appropriate ionic conductivity. However, the lithium bis (triuoromethanesulfonyl) imide (LiTFSI) SPE showed an incredibly low ionic conductivity than commercial solid electrolytes (Figure 6b). This was mainly ascribed to the poor touch between electrode and electrolyte, resulting in great resistance to ion conduction. No matter at high or low temperatures, the charge/discharge curves both showed high polarization, low capacity and poor coulomb efficiency (Figure 6c–e). As shown in Figure 6(f), both polymers

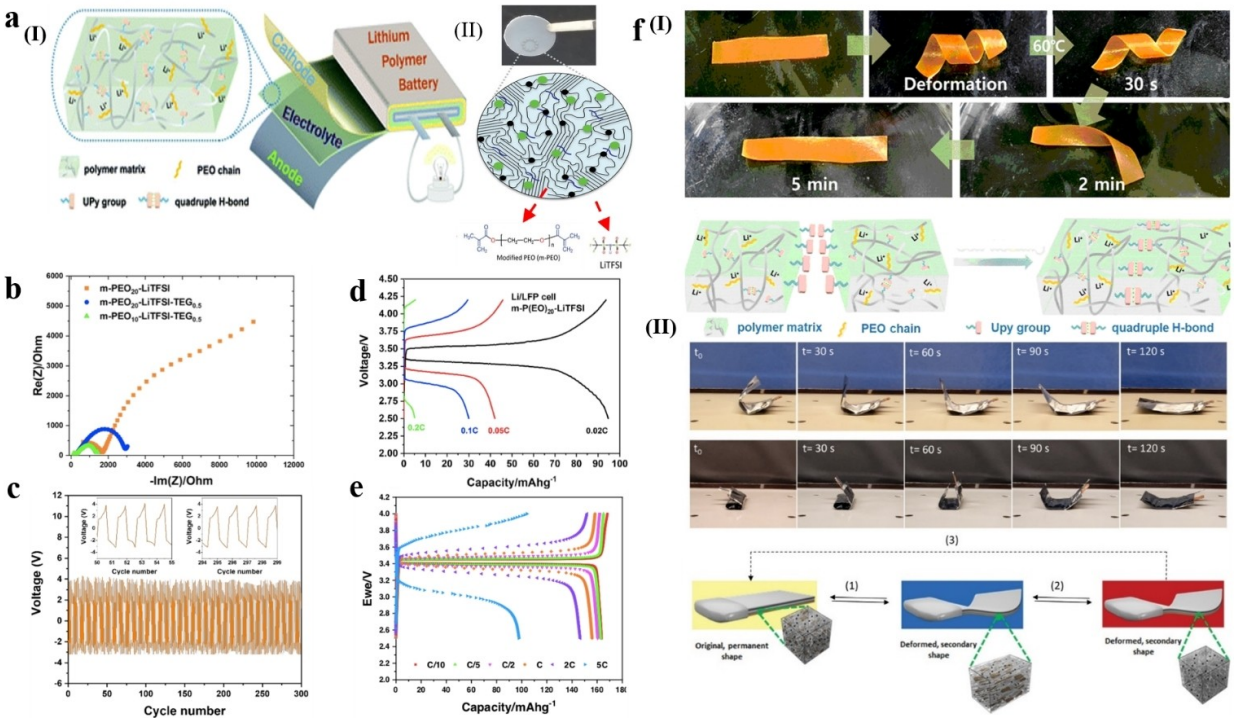

Figure 6. a) (I) Schematic diagram of PVA-UPy-PEG750 SSSPEs as solid state polymer electrolyte for LIBs. Reproduced with permission from Ref. [62]. Copyright (2019) Royal Society of Chemistry. (II) Schematic diagram of the molecular structure of SMP electrolyte. Reproduced with permission from Ref. [63]. Copyright (2021) Wiley-VCH. b) Nyquist plots of the LIBs made of the SMP electrolyte. c) Overpotential profile of Li||Li cell made with SSSPEs in applied current density. d) Voltage of Li||LFP cell made with SMP under different charge/discharge C-rates. e) Voltage profile of Li||LFP cell made with SSSPEs under different charge/discharge C-rates at 60 °C. Reproduced with permission from Ref. [63]. Copyright (2021) Wiley-VCH. f) (I) Shape recovery procedure of PVA-UPy-PEG750. Reproduced with permission from Ref. [62]. Copyright (2019) Royal Society of Chemistry. (II) Schematic illustration of shape recovery of battery from deformation. Reproduced with permission from Ref. [63]. Copyright (2021) Wiley-VCH.

performed the shape memory process very quickly, however, it is the biggest obstacle of battery performance.

There are also a lot of work on supercapacitors made from shape memory polymers. Deng et al.[64] developed a shape-memory, fiber-like supercapacitor by winding aligned CNT flakes on a SMP substrate (Figure 7a-I). Although it is elastic and stretchable, under bending and tension, the deformed shape is "frozen" as desired, and returns to its original shape when necessary. The electrochemical properties of the deformed state and the deformed state remain basically unchanged. As seen in Figure 7(b)-(I), the charge/discharge curves did not change obviously after bending with different curvature. After the material was restored to its original shape through shape memory process, CV and charge/discharge curve still had favorable effects (Figure 7c and d). Then the shape memory cycling effect was tested, and it was found that the recovery rate of 90% was achieved after electrochemical testing (Figure 7e). Zhou et al.[65] explored a healable shape-memory-based supercapacitor. In the transfer process, the conductive nanocarbon network is modified into a shape memory polymer matrix with repairing effect (Figure 7a-II). Zhong et al.[66] reported a smart shape-memory fiber supercapacitor constituted with a highly stretchable SMP substrate, MWCNT conductive layer and pseudocapacitive polyaniline layer. Similarly, Li et al.[67] prepared supercapacitors through shape memory polyurethane. Obviously, SMPs are more successful in supercapacitors than batteries. SMPs usually have low ionic conductivity. The requirement of electrolyte for ionic conductivity in supercapacitors is much lower than that in batteries. Therefore, when SMPs are used as electrolyte, they are more suitable for supercapacitors. Although SMPs have been more successful in supercapacitors than batteries, all reported supercapacitors used thermo-driven SMPs. Other 'switching' polymers may become a broader area of study.

3.3. Preliminary application

As a branch of flexible devices, shape-memory energy storage has gradually turned to the application of daily life. Liu et al.[59] designed a watchband-like supercapacitor which not only supplied power to the watch, but also maintained the shape memory property automatically induced by touching (Figure 8a). In addition, due to the good biocompatibility of Ni–Ti alloy, it was satisfactory as a surface material for long-term contact with human skin. Huang et al.[58] made smart sleeves with shape memory supercapacitors and traditional fabrics (Figure 8b). It can remember its origin shape and automatically cool when over-heated, demonstrating a potential application. Deng et al.[64] made textiles with shape memory function and energy storage using shape memory supercapacitor fibers instead of traditional yarns, and knitted clothes for dolls (Figure 8c). This smart supercapacitor is qualified as a candidate for a new generation of wearable energy storage devices.

In addition, with the advantages of energy storage devices, it can also drive gas sensors. Song et al.[68] prepared a shape memory supercapacitor with high voltage, which is integrated with a NO_2 gas sensor. This device can be connected to the skin to detect NO_2 gas without considering the folding deformation caused by elbow movement, showing its applica-

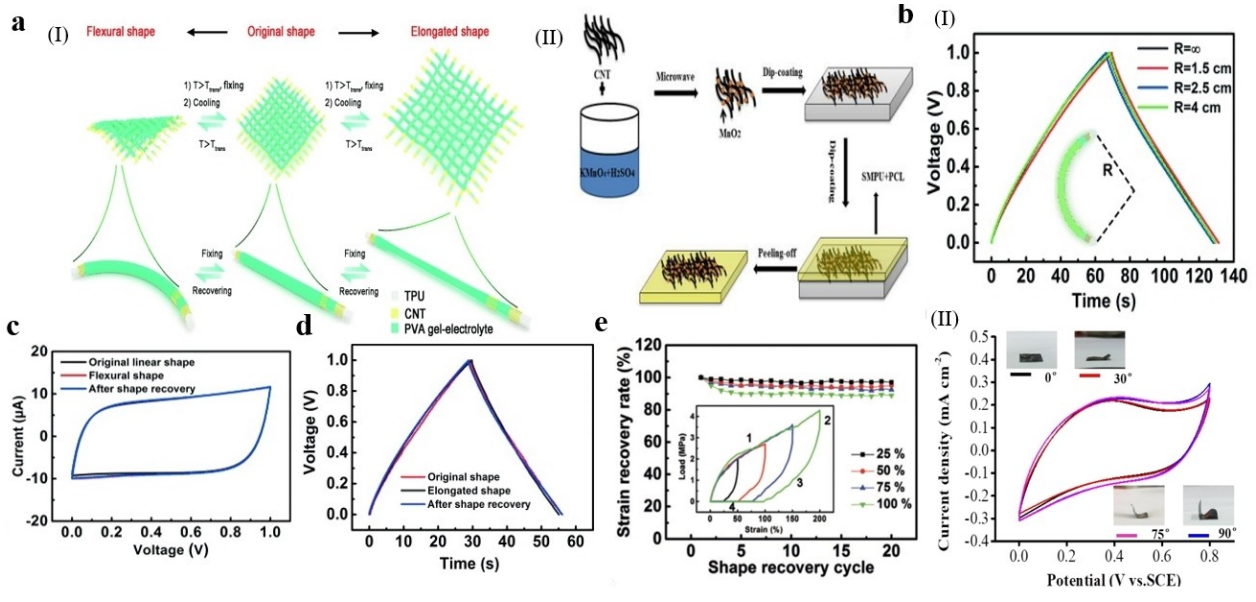

Figure 7. a) (I) Schematic diagram of SMSC and the resulting textile. Reproduced with permission from Ref. [64]. Copyright (2015) Wiley-VCH. (II) Schematic diagram of the fabrication processes of SMSC. Reproduced with permission from Ref. [65]. Copyright (2018) Multidisciplinary Digital Publishing Institute. b) (I) Charge discharge curves of SMSC under different bending shapes. Reproduced with permission from Ref. [64]. Copyright (2015) Wiley-VCH. (II) CV curves of SMSC under different bending shapes. Reproduced with permission from Ref. [65]. Copyright (2018) Multidisciplinary Digital Publishing Institute. c) CV curve before and after SMSC bending deformation and shape recovery. d) Galvanostatic charging and discharging curves of the SFSC before and after elongated deformation with a strain of 50% and shape recovery at a current density of 0.2 A g^{-1}. e) Dependence of recovery rate on shape recovery cycle for different load. Reproduced with permission from Ref. [64]. Copyright (2015) Wiley-VCH.

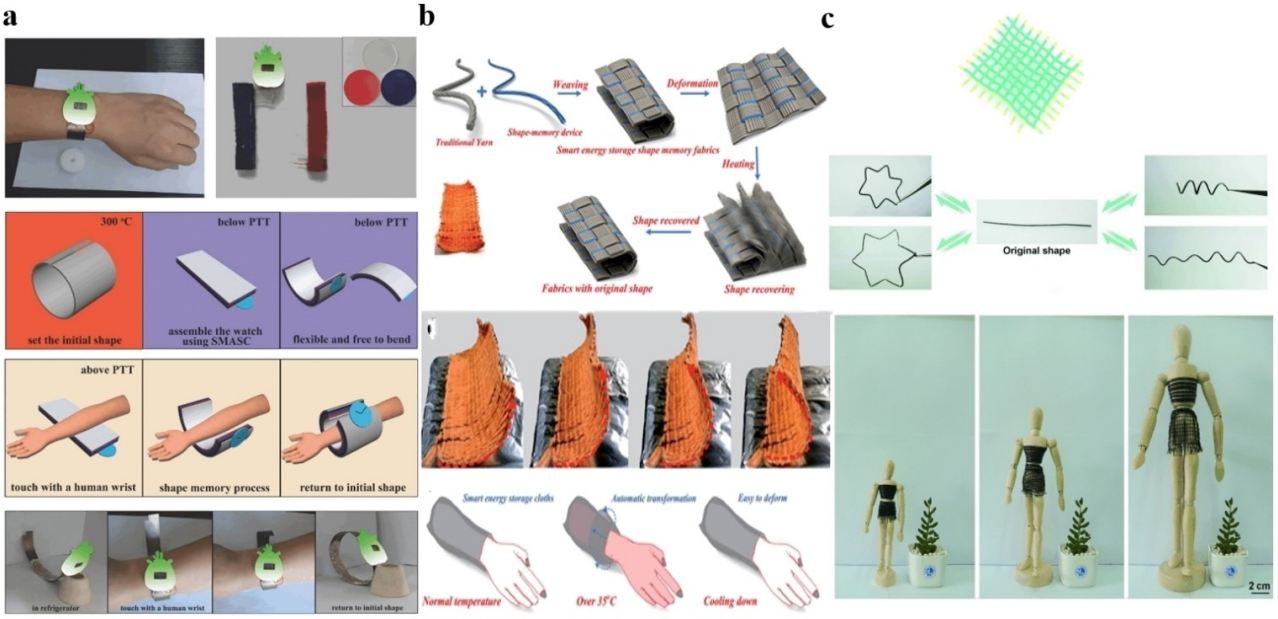

Figure 8. a) Assembled electronic watch with SMASC device as strap. Reproduced with permission from Ref. [59]. Copyright (2016) Wiley-VCH. b) SMSCs for smart textiles. Reproduced with permission from Ref. [58]. Copyright (2016) Royal Society of Chemistry. c) Smart clothing is woven from SMSCs and can be "frozen" into different shapes and sizes. Reproduced with permission from Ref. [64]. Copyright (2015) Wiley-VCH.

tion as a skin-connectable sensor device. This way of integration is a new perspective for the application of shape memory energy storage devices. More similar devices will be applied to various fields in future (detailed in Figure 9).

4. Conclusion and Perspective

As can be seen from the figure below, articles related to shape memory and flexible energy storage devices have shown an upward trend in the past decade (The data comes from Web of Science). Therefore, the integration of these two should have a prosperous application potential. Although the field of shape-memory energy storage devices is still at an early stage, there are many opportunities to be explored. We also summarized the other characteristics of the shape memory energy storage device mentioned above, hoping to provide a reference for the follow-up (Table 1). Although there have been shape-memory energy storage devices demonstrated successfully, the application scenarios are still limited. Obviously, they are mainly used in flexible and wearable devices, but new applications such as thermal management and internal triggered short circuit prepared by shape memory materials in parallel space may extend their application scope beyond flexible and wearable devices. If we can break through these boundaries and combine shape memory materials with energy storage devices more closely, shape memory energy storage devices will get greater development.

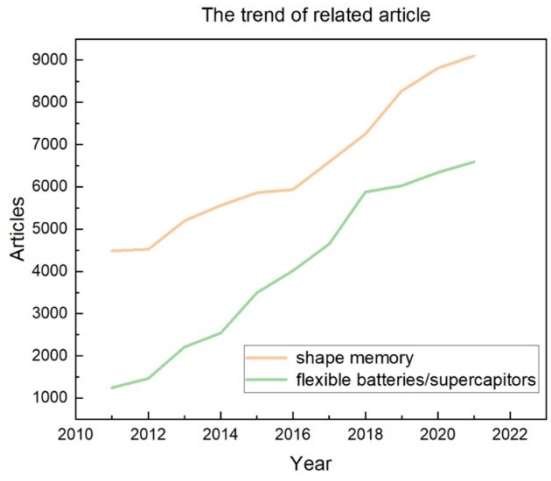

Figure 9. Trend of shape memory and flexible energy storage devices in recent ten years.

At the same time, electrochemical energy storage devices made of SMAs and SMPs still have some problems. On the one hand, most of the SMAs are used as base materials, which greatly increases the weight and volume of the battery. The kind of alloy is limited to Ni–Ti alloy, which is mainly because it is difficult to find other SMAs suitable for energy storage devices. With the continuous development of new SMAs, shape memory energy storage devices will have a breakthrough development. On the other hand, existing shape-memory energy storage devices are thermally responsive, so their performance is hampered by thermal programming and recovery steps. However, SMPs with different drivers may be a satisfactory solution to this problem. For example, the unique energy storage devices with SMPs driven by light, electricity, magnetism and solute, have a prosperous application potential. Especially in some cases, they can control the working switch

Table 1. Summary of properties and performances of shape memory batteries and supercapacitor.

Shape memory material	Function	Device	Electrodes/ electrolyte	Specific capacity	Retention	Deformation-restoration test	Other	Reference
NiTi wire	Collector	Supercapacitor	MnO_2@ NiTi MnO_2@ SS H_3PO_4-PVA gel	198.2 F/g (1 A/g)	92% (1400 cycles)	15 times 85% (shape memory recovery) 86% (capacitance retention)	25 s recover shape in 40 °C (A_s 35 °C)	[58]
NiTi flake	Collector	Supercapacitor	rGo@ NiTi MnO_2/Ni KOH-PVA gel	53.8 F/g (0.5 A/g)	86.1% (5000 cycles)	CV curves coincidence	550 s recover from 180° to 0°, 95% cell viability	[59]
NiTi wire	Collector	Battery	MnO_2/PPy@SS Zn@NiTi gelatin-borax (Zn^{2+}, Mn^{2+})	143 mAh/g (1 C)	74.2% (850 cycles)	500 times 88% (capacity retention)	6 s times in 35 °C	[55]
NiTi	Anode	Battery	Li/$NiS_{1.97}$@NiTi	540 mAh/g	_	5 times 400 mAh/g	_	[57]
MnO2/CNT/PCL/ SMPU polymer	Active material	Supercapacitor	MCPS H_2SO_4-PVA gel	27.33 mF/cm^2 (0.2 mA/cm^2)	95.02% (1500 cycles)	_	Self-healing	[65]
SMP/CNT	Electrode	Supercapacitor	SMP/CNT PVA gel	17 F/g	100% (12000 cycles)	20 times No loss for capacity	_	[64]
PVA-Upy-PEG	Electrolyte	Battery	LiFO$_4$/SPEs/Li	145 mAh/g	80.6%	_	_	[62]
m-P(EO)$_{20}$-LiTFSITEGDME$_{0.5}$	Electrolyte	Battery	Li/LiTFSI/LFP	140 mAh/g (0.2 C)	92%	100 times 92% (capacity retention)	60 °C recover	[63]

of energy storage devices by non-contact mode, or act as sensors to reflect environmental changes. This will be a very meaningful research direction and it deserves more attentions.

In addition, most of the above-mentioned shape-memory energy devices are concept verification studies rather than performance optimization studies so far. Some electrochemical energy storage devices cannot even meet the performance of daily life. Improvements in electrochemical performance are challenging, such as higher capacity and better cyclic stability, which can be achieved by optimizing the nanostructure or composition. At the same time, practical applications also require optimization of specific functions, which can be achieved through the development of new intelligent functional materials or nanostructure/composition optimization. Therefore, the balance between electrochemical performance and shape memory effect should be considered. The performance of electrochemical devices usually declines after several deformations, mainly because of the exfoliation of electrode materials and the separation of electrodes and electrolyte. To balance between shape memory effect and electrochemical performance, we should strengthen the packaging and improve the firmness of the electrode/electrolyte interface.

In summary, this is only the beginning of the development of such intelligent energy storage devices. Along this direction, a further develop booming is hoped for both research and development and commercialization of shape-memory energy storage devices.

Author Contributions

Writing-original draft preparation, L. L. Yang, Q. J. Liu, Y. F. Liu, and Y. Huang; writing-review and editing, L. L. Yang, Q. J. Liu, Y. F. Liu, and Y. Huang; supervision, Y. Huang. All the authors discussed and commented on the manuscript.

Acknowledgements

We thank the supports from the Project of International Science and Technology Cooperation in Guangdong Province (No. 2020A0505100016), the Shenzhen Sauvage Nobel Laureate Laboratory for Smart Materials, Shenzhen Science and Technology Program (No. KQTD20200820113045083, No. ZDSYS20190902093220279) and State Key Lab of Advanced Welding and Joining, Harbin Institute of Technology.

Conflict of Interest

The authors declare no conflict of interest.

Keywords: battery · energy storage · shape memory · shape memory alloys · shape memory polymers · smart material · supercapacitor

[1] M. Zhu, Y. Huang, Y. Huang, H. Li, Z. Wang, Z. Pei, Q. Xue, H. Geng, C. Zhi, *Adv. Mater.* **2017**, *29*, 160517.
[2] J. Zhang, C. P. Yang, Y. X. Yin, L. J. Wan, Y. G. Guo, *Adv. Mater.* **2016**, *28*, 9539–9544.
[3] Y. You, H. R. Yao, S. Xin, Y. X. Yin, T. T. Zuo, C. P. Yang, Y. G. Guo, Y. Cui, L. J. Wan, J. B. Goodenough, *Adv. Mater.* **2016**, *28*, 7243–7248.
[4] H. Wang, F. Li, B. Zhu, L. Guo, Y. Yang, R. Hao, H. Wang, Y. Liu, W. Wang, X. Guo, X. Chen, *Adv. Funct. Mater.* **2016**, *26*, 3472–3479.
[5] A. Manthiram, A. Vadivel Murugan, A. Sarkar, T. Muraliganth, *Energy Environ. Sci.* **2008**, *1*, 621–638.
[6] Y. Li, J. Zhang, Q. Chen, X. Xia, M. Chen, *Adv. Mater.* **2021**, *33*, e2100855.
[7] S. Koohi-Fayegh, M. A. Rosen, *J. Energy Storage* **2020**, *27*, 101047 .
[8] B. Dunn, H. Kamath, J. M. Tarascon, *Science* **2011**, *334*, 928–935.
[9] M. Armand, J. M. Tarascon, *Nature* **2008**, *451*, 652–657.
[10] N. S. Choi, Z. Chen, S. A. Freunberger, X. Ji, Y. K. Sun, K. Amine, G. Yushin, L. F. Nazar, J. Cho, P. G. Bruce, *Angew. Chem. Int. Ed. Engl.* **2012**, *51*, 9994–10024.
[11] W. Weng, P. Chen, S. He, X. Sun, H. Peng, *Angew. Chem. Int. Ed. Engl.* **2016**, *55*, 6140–6169.

[12] A. Manenti, A. Abba, A. Merati, S. M. Savaresi, A. Geraci, *IEEE Trans. Ind. Electron. Control Instrum.* **2011**, *58*, 4314–4322.
[13] H. Dai, B. Jiang, X. Hu, X. Lin, X. Wei, M. Pecht, *Renewable Sustainable Energy Rev.* **2021**, *138*, 110480.
[14] Q. Zhang, E. Uchaker, S. L. Candelaria, G. Cao, *Chem. Soc. Rev.* **2013**, *42*, 3127–3171.
[15] D. Yu, Q. Qian, L. Wei, W. Jiang, K. Goh, J. Wei, J. Zhang, Y. Chen, *Chem. Soc. Rev.* **2015**, *44*, 647–662.
[16] Y. Yang, D. Yu, H. Wang, L. Guo, *Adv. Mater.* **2017**, *29*, 1703040.
[17] R. Wang, M. Yao, Z. Niu, *InfoMat.* **2019**, *2*, 113–125.
[18] H. Sun, X. You, Y. Jiang, G. Guan, X. Fang, J. Deng, P. Chen, Y. Luo, H. Peng, *Angew. Chem. Int. Ed. Engl.* **2014**, *53*, 9526–9531.
[19] J. Li, Z. Zhou, I. Broadwell, S. Sun, *Acc. Chem. Res.* **2012**, *45*, 485–494.
[20] Y. Huang, M. Zhu, Y. Huang, Z. Pei, H. Li, Z. Wang, Q. Xue, C. Zhi, *Adv. Mater.* **2016**, *28*, 8344–8364.
[21] Z. Xu, *shape memory material*, Shanghai Jiaotong University Press, Shanghai **2000**.
[22] P. Yang, F. Zhu, Z. Zhang, Y. Cheng, Z. Wang, Y. Li, *Chem. Soc. Rev.* **2021**, *50*, 8319–8343.
[23] L. Sun, W. M. Huang, Z. Ding, Y. Zhao, C. C. Wang, H. Purnawali, C. Tang, *Mater. Des.* **2012**, *33*, 577–640.
[24] G. Costanza, M. E. Tata, *Materials* **2020**, *13*, 1856.
[25] M. Hao, J. Li, S. Park, S. Moura, C. Dames, *Nat. Energy* **2018**, *3*, 899–906.
[26] M. Zhang, J. Du, L. Liu, A. Stefanopoulou, J. Siegel, L. Lu, X. He, X. Xie, M. Ouyang, *J. Electrochem. Soc.* **2017**, *164*, A3038–A3044.
[27] S. C. Kwon, S. H. Jeon, H. U. Oh, *Cryogenics* **2015**, *67*, 19–27.
[28] Z. G. Wei, R. Sandstroröm, S. Miyazaki, *J. Mater. Sci.* **1998**, *33*, 3743–3762.
[29] Y. Xia, Y. He, F. Zhang, Y. Liu, J. Leng, *Adv. Mater.* **2021**, *33*, e2000713.
[30] A. Lendlein, O. Gould, *Nat. Rev. Mater.* **2019**, *4*, 116–133.
[31] T. Nguyen, H. Jerryqi, F. Castro, K. Long, *J. Mech. Phys. Solids* **2008**, *56*, 2792–2814.
[32] Z. D. W. M. Huang, C. C. Wang, J. Wei, Y. Zhao, H. Purnawali, *Mater. Today* **2010**, *13*, 7–8.
[33] M. Behl, A. Lendlein, *Mater. Today* **2007**, *10*, 20–28.
[34] C. D. Wick, A. J. Peters, G. Li, *Polymer* **2021**, *213*, 123319.
[35] Y. Liu, K. Gall, M. L. Dunn, A. R. Greenberg, J. Diani, *Int. J. Plast.* **2006**, *22*, 279–313.
[36] M. Elahinia, N. Shayesteh Moghaddam, M. Taheri Andani, A. Amerinatanzi, B. A. Bimber, R. F. Hamilton, *Prog. Mater. Sci.* **2016**, *83*, 630–663.
[37] X. Chen, K. Liu, W. Guo, N. Gangil, A. N. Siddiquee, S. Konovalov, *Rapid Prototyping J.* **2019**, *25*, 1421–1432.
[38] K. K. Alaneme, J. U. Anaele, E. A. Okotete, *Sci. Afr.* **2021**, *12*, e00760.
[39] A. Agrawal, R. K. Dube, *J. Alloys Compd.* **2018**, *750*, 235–247.
[40] H. Peng, J. Chen, Y. Wang, Y. Wen, *Adv. Eng. Mater.* **2018**, *20*, 1700741.
[41] J. Shang, X. Le, J. Zhang, T. Chen, P. Theato, *Polym. Chem.* **2019**, *10*, 1036–1055.
[42] M. J. Haskew, J. G. Hardy, *Johnson Matthey Technol. Rev.* **2020**, *64*, 425–442.
[43] Y. Zhang, M. S. Desai, T. Wang, S. W. Lee, *Biomacromolecules* **2020**, *21*, 1149–1156.
[44] Y. N. Chen, L. Peng, T. Liu, Y. Wang, S. Shi, H. Wang, *ACS Appl. Mater. Interfaces* **2016**, *8*, 27199–27206.
[45] X. Wan, F. Zhang, Y. Liu, J. Leng, *Carbon* **2019**, *155*, 77–87.
[46] H. Lu, Y. Liu, J. Gou, J. Leng, S. Du, *Compos. Sci. Technol.* **2011**, *71*, 1427–1434.
[47] P. Wang, S. Liu, S. Chen, H. Liu, Y. Wu, L. Liu, *Mater. Lett.* **2018**, *220*, 297–300.
[48] F. H. Zhang, Z. C. Zhang, C. J. Luo, I. T. Lin, Y. Liu, J. Leng, S. K. Smoukov, *J. Mater. Chem. C* **2015**, *3*, 11290–11293.
[49] Q. Ze, X. Kuang, S. Wu, J. Wong, S. M. Montgomery, R. Zhang, J. M. Kovitz, F. Yang, H. J. Qi, R. Zhao, *Adv. Mater.* **2020**, *32*, e1906657.
[50] H. Zhang, Y. Zhao, *ACS Appl. Mater. Interfaces* **2013**, *5*, 13069–13075.
[51] H. Zhang, J. Zhang, X. Tong, D. Ma, Y. Zhao, *Macromol. Rapid Commun.* **2013**, *34*, 1575–1579.
[52] X. Zhang, C. Zhu, B. Xu, L. Qin, J. Wei, Y. Yu, *ACS Appl. Mater. Interfaces* **2019**, *11*, 46212–46218.
[53] H. Chen, Y. Li, Y. Liu, T. Gong, L. Wang, S. Zhou, *Polym. Chem.* **2014**, *5*, 5168–5174.
[54] Y. Cui, D. Li, C. Gong, C. Chang, *ACS Nano* **2021**, *15*, 13712–13720.
[55] Z. Wang, Z. Ruan, Z. Liu, Y. Wang, Z. Tang, H. Li, M. Zhu, T. F. Hung, J. Liu, Z. Shi, C. Zhi, *J. Mater. Chem. A* **2018**, *6*, 8549–8557.
[56] G. B. Cho, S. S. Jeong, S. M. Park, T. H. Nam, *Mater. Sci. Forum* **2005**, *486–487*, 650–653.
[57] G.-b. Cho, K.-w. Kim, H.-j. Ahn, K.-k. Cho, T.-H. Nam, *J. Alloys Compd.* **2008**, *449*, 317–321.
[58] Y. Huang, M. Zhu, Z. Pei, Q. Xue, Y. Huang, C. Zhi, *J. Mater. Chem. A* **2016**, *4*, 1290–1297.
[59] L. Liu, B. Shen, D. Jiang, R. Guo, L. Kong, X. Yan, *Adv. Energy Mater.* **2016**, *6*, 1600763.
[60] Z. Zhao, Q. Liu, L. Zang, H. You, J. Zhang, X. Wang, C. Yang, *J. Alloys Compd.* **2021**, *888*, 161646.
[61] B. Zhou, D. He, J. Hu, Y. Ye, H. Peng, X. Zhou, X. Xie, Z. Xue, *J. Mater. Chem. A* **2018**, *6*, 11725–11733.
[62] Y. H. Jo, B. Zhou, K. Jiang, S. Li, C. Zuo, H. Gan, D. He, X. Zhou, Z. Xue, *Polym. Chem.* **2019**, *10*, 6561–6569.
[63] V. Jabbari, V. Yurkiv, M. G. Rasul, M. Cheng, P. Griffin, F. Mashayek, R. Shahbazian-Yassar, *Small* **2022**, *18*, e2102666.
[64] J. Deng, Y. Zhang, Y. Zhao, P. Chen, X. Cheng, H. Peng, *Angew. Chem. Int. Ed. Engl.* **2015**, *54*, 15419–15423.
[65] H. Zhou, H. Luo, X. Zhou, H. Wang, Y. Yao, W. Lin, G. Yi, *Appl. Sci.* **2018**, *8*, 1732.
[66] J. Zhong, J. Meng, Z. Yang, P. Poulin, N. Koratkar, *Nano Energy* **2015**, *17*, 330–338.
[67] T. Li, X. Fang, Q. Pang, W. Huang, J. Sun, *J. Mater. Chem. A* **2019**, *7*, 17456–17465.
[68] C. Song, J. Yun, H. Lee, H. Park, Y. R. Jeong, G. Lee, M. S. Kim, J. S. Ha, *Adv. Funct. Mater.* **2019**, *29*, 1901996.

Manuscript received: June 20, 2022
Revised manuscript received: July 28, 2022
Version of record online: August 29, 2022